

Light-induced superconductivity in a strongly correlated electron system

Nikolaj Bittner,¹ Takami Tohyama,² Stefan Kaiser,^{1,3} and Dirk Manske¹

¹*Max-Planck-Institut für Festkörperforschung, D-70569 Stuttgart, Germany*

²*Department of Applied Physics, Tokyo University of Science, Tokyo 125-8585, Japan*

³*4th Physics Institute, University of Stuttgart, D-70569 Stuttgart, Germany*

We present a theoretical study of possible light-induced superconducting phase coherence in a solid state system after an ultrafast optical excitation. We investigate the buildup of superconducting correlations by calculating an exact time-dependent wave function reflecting the properties of the system in non-equilibrium and the corresponding transient response functions. Dynamically quenching the non-superconducting wavefunction a characteristic superfluid density emerges and a transient Meissner effect appears that we compare to experimental data. In particular, we find that the stability of the induced superconducting state depends crucially on the nature of the excitation quench: namely, a pure interaction quench induces a long-lived superconducting state, whereas a phase quench leads to a short-lived transient superconductor.

Introduction. Recent developments of ultrashort laser pulses allow for optical control of the complex matter on picosecond time-scales. Intriguing experiments at mid-IR and THz frequency ranges reported controlling non-equilibrium superconductivity [1–6]: Tailored excitation pulses tuned resonantly to specific phonon modes have been shown to induce transient superconducting states far above equilibrium transition temperature (T_c). This goes beyond the typical photo-doping experiments [7, 8], where the superconducting condensate is broken by ultrashort near IR pulses. So far the experiments with light-induced superconductivity can be roughly divided into two classes [9]. On the one hand superconductivity can emerge after suppression of a competing order. Here, the key experiment was performed via phonon pumping on 1/8 doped LESCO [1, 2], where superconductivity is fully suppressed due to the appearance of a competing stripe order stabilized by lattice distortion. Melting competing stripes with a light pulse allows for the reappearance [1, 2] and enhancement [10, 11] of the superconductivity. This picture was also supported by theoretical investigations [12, 13], where the *existing* superconductivity was enhanced after suppressing competing orders by optical pulses. However, most intriguing are experiments that really *induce* superconducting coherence into the electron system. That allows stabilizing superconducting state far above T_c [3–6]; Most prominent in YBCO that was possible throughout the pseudogap phase and even up to room temperature for very underdoped samples [3, 5]. Key to these experiments is the resonant pumping of the c -axis infrared-active CuO mode, which basically modulates apical oxygen displacement from the CuO planes, leading to a redistribution of the interlayer coherence between the planes [4]; Although the evidence for the competing order of the incommensurate CDW in YBCO was found [14], the temperature and time dependent measurements rules out its melting as a key element of inducing superconductivity. A leading idea emphasizing the role of phonon pumping is based on the displacement of the lattice structure through non-linear phononics [15, 16]. This transient structure frozen at maximum lattice displacement suggests an enhanced superconducting coupling strength [17]. However, comparing with theoretical expectations the transient displacement and therefore impact of this effect seems rather small to explain the observed enhanced T_c . Explanations going beyond the structure dynamics are focusing on the amplification of the *existing* electron pairing either by changing of microscopic parameters responsible for superconductivity [18–21], by parametric cooling [22] or by phononic squeezing [23, 24]. Though, none of them describe the possibility to induce superconducting coherence. An important experimental aspect, which was so far disregarded, is the possibility of the modulated effective interactions after an optical excitation. The significance of such modulations was experimentally shown on 1D organic molecules [25, 26], where a controlled change in Coulomb interaction U was achieved, and most spectacular is discussed as a key element for possible light-induced superconductivity in K-doped C_{60} [6, 27, 28]. In the latter case, a transient superconducting state was observed after a tailored optical pulse, which modulates the local charge density. However, the understanding of the microscopic mechanism for the observed superconducting signatures in nonequilibrium is still missing.

Following that view we propose here a general concept to induce nonequilibrium electronic phase coherence after an optical excitation (see Fig. 1) by emphasizing the role of modulated correlations U/t_h . In particular, we show the possibility of light-induced superconducting coherence following two basic concepts: namely, pulse stimulated changes in the interaction strength of the electron system (e.g. on-site U) and modification of the electron hopping $t_h \exp(iA(t))$ by the time-dependent vector potential $A(t)$ of the light field. To capture the essential physics we simulate an electron system in nonequilibrium by the extended Hubbard model (EHM) with an additional next neighbor interaction V in one dimension (1D) at half-filling [29–31] described by the time-dependent Hamiltonian:

$$\hat{H}(t) = \underbrace{-t_h e^{iA(t)} \sum_{i\sigma} \left(\hat{c}_{i,\sigma}^\dagger \hat{c}_{i+1,\sigma} + \text{H.c.} \right)}_{\text{(II) phase quench}} + \underbrace{[U + \Delta U \Theta(t)] \sum_i \hat{n}_{i\uparrow} \hat{n}_{i\downarrow} + [V + \Delta V \Theta(t)] \sum_i \hat{n}_i \hat{n}_{i+1}}_{\text{(I) interaction quench}}, \quad (1)$$

where $\hat{c}_{i,\sigma}^\dagger$ ($\hat{c}_{i,\sigma}$) represents creation (annihilation) operator for one electron with spin $\sigma = \uparrow, \downarrow$ at site i . Here, the occupation number operator is given by $\hat{n}_i = \hat{n}_{i\uparrow} + \hat{n}_{i\downarrow}$ with $\hat{n}_{i\sigma} = \hat{c}_{i,\sigma}^\dagger \hat{c}_{i,\sigma}$. The transient dynamics of the system is modeled in the following way: Before the excitation (at negative time delays) we prepare the system in equilibrium ground state (GS) of the CDW (see Fig. 1(a)). Then, at $t = 0$ the laser pulse arises, which leads to either (I) abrupt changing interaction parameters on the diagonal of the Hamiltonian (1) (green part in Fig. 1(b))

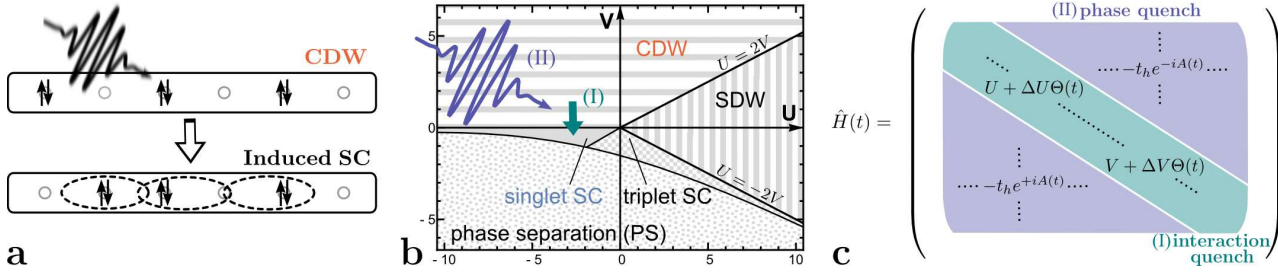


Figure 1. (color online) (a) Inducing phase coherence with an optical pulse. Here, spatial distribution of electrons on a lattice before and after pulse corresponds to CDW and singlet SC, respectively. (b) Illustration of the equilibrium phase diagram for the 1D EHM at half filling ($T=0$) with U and V being the strength of the on-site and nearest neighbor interaction from Eq. (1), respectively. Here, each shaded region corresponds to a particular phase from EHM. The nonequilibrium transition between phases is initiated by an optical pulse following two scenarios: (I) an interaction quench or (II) a phase quench. (c) Illustration of the time-dependent Hamiltonian Matrix. While after interaction quench the diagonal part of the Hamiltonian (green) is changed, phase quench modifies its off-diagonal part (blue).

and (c)) or (II) to modification of the hopping by the time-dependent vector potential $A(t)$ of the light field on its off-diagonals (blue part in Fig. 1(b) and (c)). Both drive the system out of equilibrium and induces transient superconducting state. To examine how light-induced phase coherence emerges and the system evolves toward superconductivity (Fig. 1(a)), we use Lanczos based exact diagonalization (see Methods).

Numerical results

Induced phase coherence due to interaction quench. Light-induced abrupt change in the interaction strength of the electron system leads to the modification in the eigenstates of the system and, in turn, to the redistribution of the electrons on a lattice. To visualize this process we have calculated the excitation spectrum of the system in nonequilibrium and compared it with its equilibrium counterparts before and after quenching (see Fig. 2(a)). Here, we prepare the system at $t < 0$ in equilibrium ground state (GS) with $U = -4, V = 0.25$

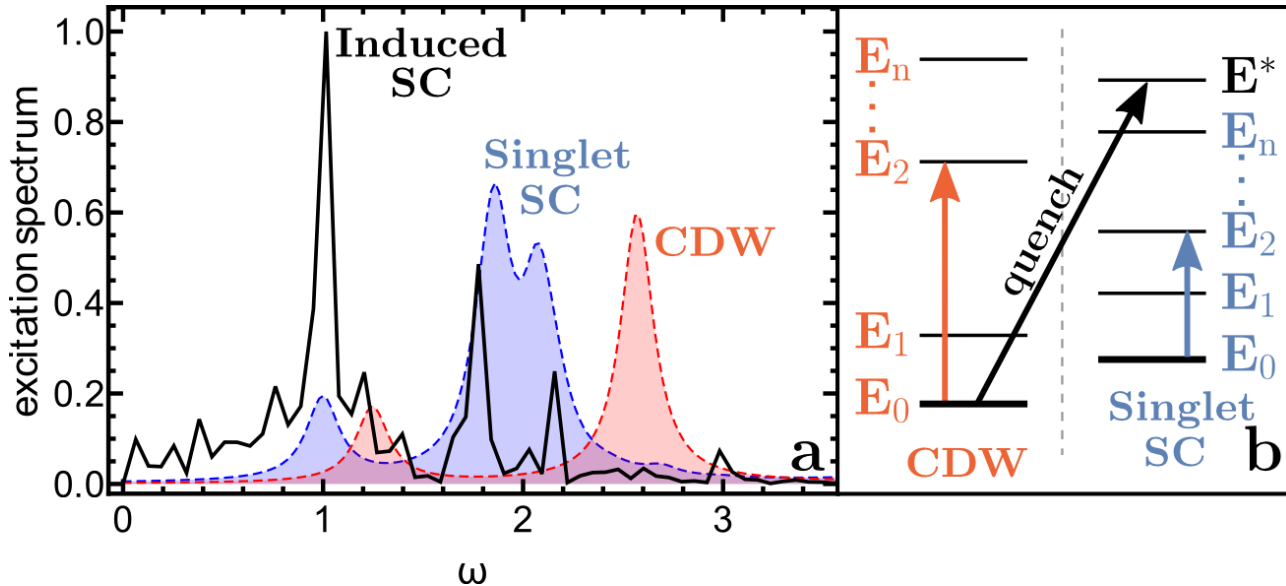


Figure 2. (color online) (a) Excitation spectrum of the system in nonequilibrium (black solid line) compared with the spectra in equilibrium singlet SC phase (blue region) and equilibrium CDW phase (red region). (b) Schematic illustration of the interaction quench together with excitation processes in SC and CDW phases. Energy levels in both phases are presented by the black bars. A nonequilibrium state is indicated by E^* .

corresponding to the CDW phase and switch abruptly at $t = 0$ the nearest neighbor interaction parameter V into the superconducting region with $V = -0.25$. Thus, the strongly correlated electron system evolves for $t > 0$ under perturbed Hamiltonian with the modified diagonal part (see Fig. 1(c)). Analyzing the excitation spectrum in nonequilibrium (black line) in Fig. 2(a) we can draw some important conclusions. First of all, there are no peaks in spectrum, which could be identified with the equilibrium CDW phase (red area). Moreover, the most intensive peaks in spectrum correspond to the low-energy excited states in the equilibrium SC phase (blue area). Finally, since the interaction quench is a nonadiabatic process, the system does not appear in the ground state of the singlet SC phase after quenching, but in some nonequilibrium state E^* . Physically that means, that after quenching the system goes directly into a nonequilibrium state in the SC phase and the CDW is fully suppressed, as schematically summarized in Fig. 2(b).

To show how superconducting signatures emerges after interaction quench with time, we calculate correlation functions and more significantly the experimentally relevant time-dependent optical conductivity $\sigma(\Delta t, \omega)$ with Δt being the time delay between the pump and probe pulses (see Methods). First we plot in Fig. 3(a) and (b) time-dependent density-density $C(j, t)$ and on-site $P_1(j, t)$ correlation functions, which characterize the temporal evolution of the charge order and of the superconducting correlations, respectively. Clearly, the charge density wave state prepared at $t < 0$ and showing characteristic "zigzag" structure in Fig. 3(a) is strongly suppressed after quenching. At the same time, the on-site correlation function $P_1(j, t)$ presented in Fig. 3(b)

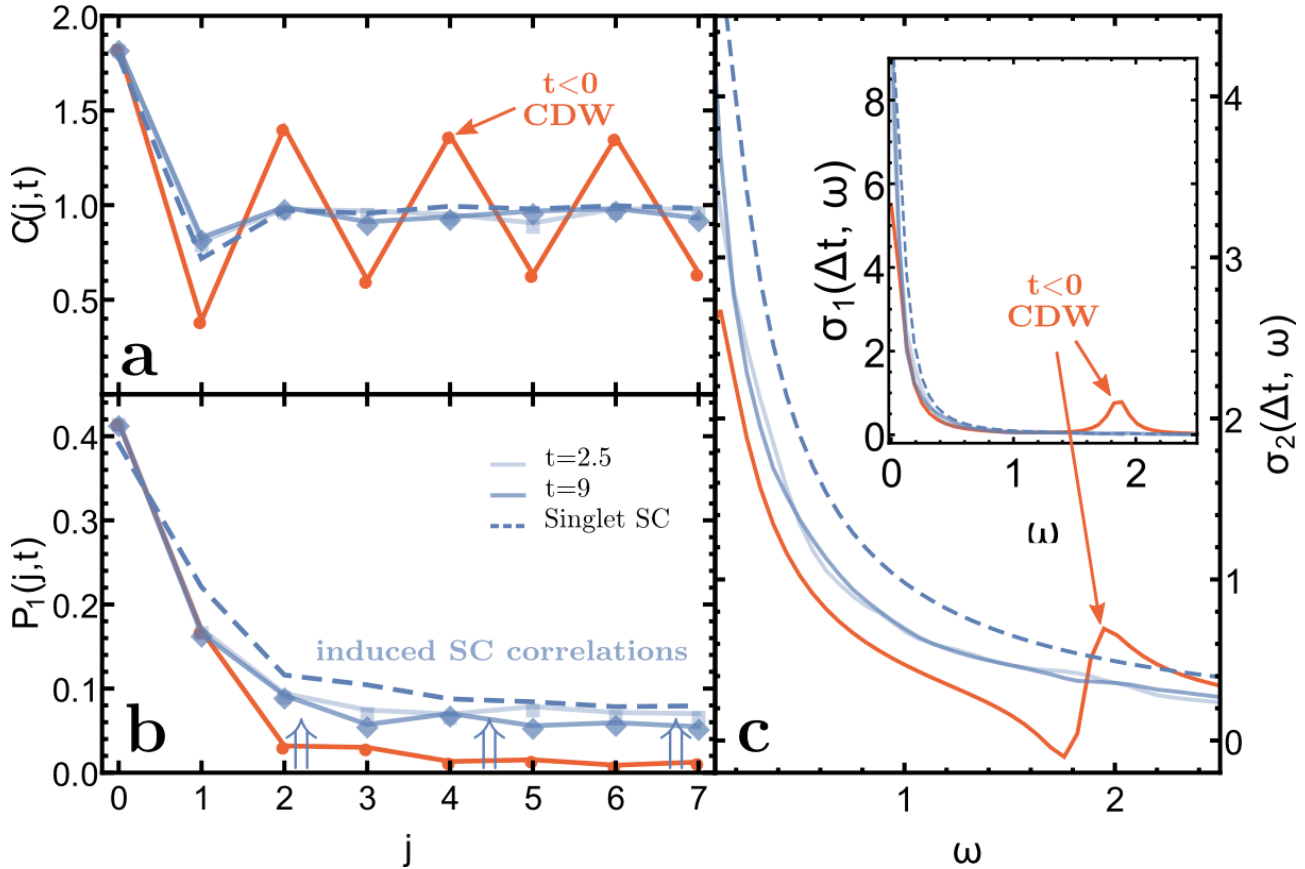


Figure 3. (color online) Time-dependent (a) density-density and (b) singlet superconducting correlation functions for 14-site lattice obtained for the interaction quench ($U = -4$, $V = 0.25$, $\Delta V = -0.5$). The functions are exemplary shown at times: $t = 0$ (red solid line), $t = 2.5$ (light blue solid line) and $t = 9$ (blue solid line). For comparison, the correlation functions in equilibrium singlet SC phase are indicated by blue dashed lines. (c) The calculated corresponding imaginary optical conductivity $\sigma_2(\Delta t, \omega)$. Its real part $\sigma_1(\Delta t, \omega)$ is shown in inset.

shows strong enhancement of the superconducting correlations in nonequilibrium. Moreover, a direct comparison of $P_1(j, t)$ in nonequilibrium with the result for equilibrium superconducting GS (blue dashed line) reveals a quite good agreement. Finally, we focus on a time-dependent optical conductivity quantity $\sigma(\Delta t, \omega)$. Superconductivity is identified in the complex $\sigma(\Delta t, \omega)$ as follows: Due to the perfect diamagnetic response of a superconductor the imaginary part $\sigma_2(\Delta t, \omega)$ diverges with a characteristic Landau $1/\omega$ -behavior for $\omega \rightarrow 0$ indicating the Meissner effect. The perfect conductivity leads in the real part $\sigma_1(\Delta t, \omega)$ to the opening of a superconducting gap of the optical conductivity and a transfer of the spectral weight into the zero frequency δ -peak. In Fig. 3(c) we show the imaginary and real (inset) parts of the optical conductivity calculated in equilibrium superconducting state (blue dashed line) and after quenching (solid lines). Clearly, after quenching $\sigma_2(\Delta t, \omega)$ shows disappearance of the CDW response visible as clear spectral feature $\omega \approx 1.8$ in the equilibrium spectra (red solid line) and the appearance of a clear inductive response with a superconducting-like $1/\omega$ behavior in the transient spectra (blue solid lines). That indicates the emergence of the superconducting correlations via the Meissner effect. Equivalent indications were also found in the temporal evolution of $\sigma_1(\Delta t, \omega)$ (inset in Fig. 3(c)), where the spectral weight of the low energy peak at $\omega \approx 1.8$ corresponding to the equilibrium CDW state is shifted after quenching into the low-energy peak at $\omega \approx 0$ representing a transient δ -peak.

Realistic phase quench and comparison with experiment. As discussed in the introduction we investigate now the second important case, where a light pulse modifies the electron hopping with the possibility to induce phase coherence between the electron pairs on the lattice. To examine the behavior of the system after pumping we calculated the projection of the time-dependent wave function $|\psi(t)\rangle$ from Eq. (2) to ground states $|0\rangle$ in different phases (see Fig. 4 (a)). Here, the system is initially prepared in the GS with $U = -3, V = 0.5$ corresponding to the CDW phase and at $t = 0$ gets exposed to the light field with a finite width according to Eq. (1) (blue part). The central frequency of the pulse is tuned to the first low-energy excited state in the CDW phase to guarantee an effective transfer of the pulse energy to electrons and to avoid excessive pumping of the system. The duration time of the pump pulse we set to $\tau = 0.05$ in order to reach simultaneously different excited states of the system. As can be clearly seen in Fig. 4 (a), after pumping the CDW component in the time-dependent wave function is only partially suppressed (red solid line), whereas the projection to the superconducting ground state (blue solid line) shows a temporal enhancement in the overlap function $|\langle\psi(t)|0\rangle|^2$. Moreover, at $t \approx 7$ the overlap with the ground state in the superconducting phase is even larger, than with the

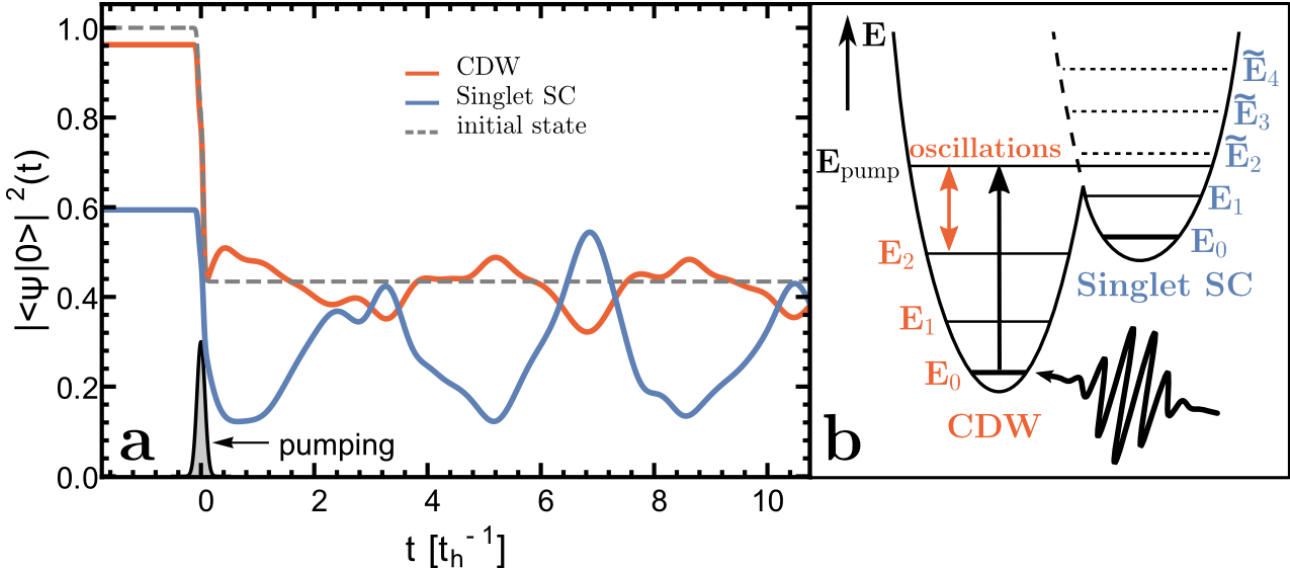


Figure 4. (color online) (a) Projection of the time-dependent wave function $|\psi(t)\rangle$ to the ground states $|0\rangle$ with parameters: $U = -3$ and $V = 0.7$ (CDW), -0.5 (Singlet SC), and 0.5 (initial state). Here, the system is excited by the pulse of a Gaussian shape, which is indicated by the black region around $t = 0$ and has parameters: $A_0=5$, $\omega=2.38$, $\tau=0.05$. (b) Illustration of the processes in a system after its interaction with a strong light pulse.

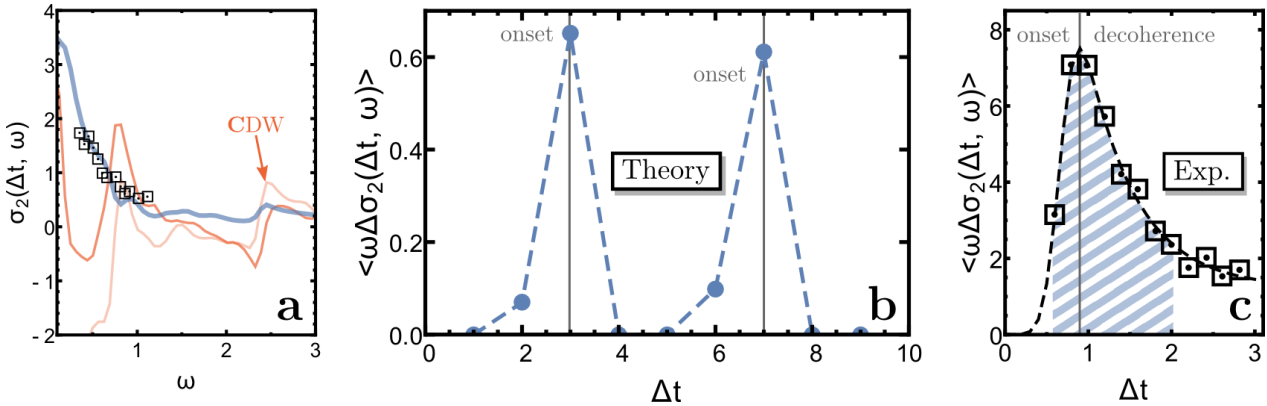


Figure 5. (color online) (a) Time-dependent imaginary conductivity $\sigma_2(\Delta t, \omega)$. Theoretically obtained results at different time delays are presented by the solid lines: $\Delta t=1$ (light red), $\Delta t=2$ (red), and $\Delta t=3$ (blue), whereas experimentally measured data for YBCO 6.45 at $T = 100\text{K}$ are shown by the black squares. (b) Theoretically calculated for the Hubbard model and (c) experimentally measured [5] for YBCO 6.45 at $T = 100\text{K}$ transient value of $\langle \omega \sigma_2(\Delta t, \omega) \rangle$ for different time delays Δt . The gray solid lines separating onset and decoherence areas on figures serve as guides to the eye.

initial state (gray dashed line). In other words, after pumping the system is excited to some joint state of the CDW and SC, as illustrated in Fig. 4(b) and a dynamical coexistence of both phases is therefore possible. This interpretation is also supported by the excitation spectrum and correlation function (shown in Supplemental Material).

To explore the temporal dynamics of this joint state and, in particular, buildup of the superconducting phase coherence, we calculate the time-dependent optical conductivity (see Fig. 5). In Fig. 5(a) we show first the imaginary conductivity $\sigma_2(\Delta t, \omega)$ (the real part $\sigma_1(\Delta t, \omega)$ is presented in the Supplemental Material), where we observe a reduction of the equilibrium low-energy CDW response at both $t = 1$ (light red line) and $t = 2$ (red line) with the appearance of an in-gap state at $\omega \approx 0.7$. Physically this could be interpreted that laser pumping creates some photo-carriers, which remain localized on the lattice throughout the still existing CDW excitations. Subsequently, at $t = 3$ (blue line) the response from CDW is disappeared and the system shows a characteristic Landau $1/\omega$ -like behavior. This we attribute as the diamagnetic response emerging from the superconducting correlation due to the Meissner effect. Moreover, a comparison with experimental results reveals a quite good agreement of the induced inductive response shown exemplary for the cuprate YBCO 6.45 under phonon pumping [5] (open black squares). We note that a $1/\omega$ behavior is a generic characteristics found throughout induced superconductors [1, 3, 6, 10]. Finally, to characterize the superfluid density we calculate $\omega \sigma_2(\Delta t, \omega)$ by fitting the $1/\omega$ divergence at low frequencies for each spectrum. Fig. 5(b) shows the extracted transient superfluid density as a function of time delay Δt between pump and probe pulses. Pumping the system with a light pulse clearly leads to an induction of a finite superfluid density with an onset between $\Delta t = 1$ to 3. On the other hand, the dynamical coexistence of the charge density wave and superconducting excitations leads to the characteristic oscillating behavior discussed above. This is also seen in the reappearing onset in $\omega \sigma_2(\Delta t, \omega)$ between $\Delta t = 5$ to 7. Hence, the transient character of the wave function (see Fig. 4(a)) describes a periodic decoherence and therefore leads to a short-lived transient superconducting state. Experimentally a similar onset of the induced superfluid density is also found in the above mentioned cuprate YBCO 6.45 as shown in Fig. 5(c). The stability of the experimentally induced superconductor is limited by decoherence leading to a short-lived transient state [5] as well.

Conclusion. In the present paper we have demonstrated the possibility that tailored light pulses that modulate correlations are able to induce superconducting phase coherence in transient nonequilibrium states. Both in the correlation functions, excitation spectra and in the transient wavefunction we find clear evidences for the transient superconducting response in the light induced state. Also calculating the transient ac-optical conductivity reveals a clear superconducting response in the driven state by transferring spectral weight into the superconducting zero frequency δ -peak in the real part of the optical conductivity and the characteristic

$1/\omega$ divergence of the low frequency imaginary conductivity due to the Meissner effect. The latter allows us extracting the induced superfluid densities and a comparison with experimental quantities. Our comprehensive picture interprets this inductive response as a transient Meissner effect, since it clearly emerges from the induced superconducting correlations and excitations. Based on the quench processes the induced nonequilibrium states show distinct different transient behaviors. While for a pure interaction quench a long-lived superconducting state can be induced, for a phase quench a short-lived transient superconducting state emerges.

Acknowledgment. The authors are grateful to A. Schnyder, A. Cavalleri, and H. Krull for helpful discussions. N.B. thanks the YITP in Kyoto, Japan for its hospitality.

Methods.

Model definition. The excitation of the system occur by a light pulse, which can be incorporated into the Hamiltonian in two different ways: (I) by interaction quench and (II) by phase quench (see Fig. 1). In case (I) one deals with a quite simple and popular type of the quantum quench protocol [32], where at a fix moment in time the interaction strength parameters U and V are abruptly changed by ΔU and ΔV . The situation (II) represents excitation of an electron system with a light pulse with a finite duration time. The electromagnetic field is included into the Hamiltonian by means of the Peierls substitution. The pulse is modeled in the temporal gauge by a spatially uniform, but time-dependent vector potential $A(t) = A_0 e^{-t^2/2\tau^2} \cos(\omega_{\text{pump}} t)$, with A_0 being the amplitude of the laser field, ω_{pump} representing the frequency of the pulse, and τ denoting its full width at half maximum. The vector potential $A(t)$ reaches its maximum at $t = 0$. The temporal evolution of the interacting electron system obeys the Schrödinger equation, which we numerically solve by employing the time-dependent Lanczos method [33]. Its general idea consists in the stepwise application of the Lanczos algorithm in time intervals δt . At each time step $t + \delta t$ Lanczos method generates a tridiagonal matrix with the eigenvectors $|\phi_l\rangle$ and corresponding eigenvalues ϵ_l . These results are subsequently used to approximate the time-dependent wave function, which then reads:

$$|\psi(t+\delta t)\rangle \approx e^{-i\hat{H}(t)\delta t} |\psi(t)\rangle \approx \sum_{l=1}^M e^{-i\epsilon_l \delta t} |\phi_l\rangle \langle \phi_l | \psi(t)\rangle \quad (2)$$

Correlation and response functions. Based on the knowledge of the time-dependent wave function from Eq. (2) we calculate correlation functions as well as optical conductivity, which are good quantities to examine a contrast between two neighboring CDW and SC phases. The temporal evolution of the charge order can be traced by the time-dependent density-density correlations function, which for each lattice site j reads

$$C(j, t) = \frac{1}{L} \sum_{l=0}^{L-1} \langle \psi(t) | \hat{n}_{l+j} \hat{n}_l | \psi(t) \rangle \quad (3)$$

with L being the lattice size. In analogy, to investigate the time-dependent behavior of the singlet superconducting correlations we introduce the on-site correlation function:

$$P_1(j, t) = \frac{1}{L} \sum_{l=0}^{L-1} \left\langle \psi(t) \left| \hat{c}_{l+j\downarrow}^\dagger \hat{c}_{l+j\uparrow}^\dagger \hat{c}_{l\uparrow} \hat{c}_{l\downarrow} \right| \psi(t) \right\rangle . \quad (4)$$

It should be noted that at $j = 0$ this function represents the double occupancy function. To calculate the optical pump-probe conductivity $\sigma(\Delta t, \omega)$, we introduce into our calculations an additional probing pulse described by $A_{\text{pr}}(\Delta t, t)$ at time delay Δt , which is assumed to be weak and short in time. For a given pump we then sequentially calculate the time-dependent current density without and with an additional probe pulse. The difference in both results gives the current density $j_{\text{pr}}(\Delta t, t)$ induced by the probing excitation. Finally, the optical conductivity is calculated from the Fourier transformation of $j_{\text{pr}}(\Delta t, t)$ and the $A_{\text{pr}}(\Delta t, t)$ with respect to t :

$$\sigma(\Delta t, \omega) = \frac{j_{\text{pr}}(\Delta t, \omega)}{i(\omega + i\eta) L A_{\text{pr}}(\Delta t, \omega)} . \quad (5)$$

For the broadening of the spectral lines we added artificially a small positive number $\eta = 1/L$.

For the numerical calculations, we use 10-site lattice with periodic boundary conditions and set hopping parameter $t_h = 1$. Further, we measure the energy and time in units t_h and t_h^{-1} , respectively. For the Lanczos method we take $M = 40$ iterations. The time interval is set to $\delta t = 0.01$.

-
- [1] D. Fausti, R. I. Tobey, N. Dean, S. Kaiser, A. Dienst, M. C. Hoffmann, S. Pyon, T. Takayama, H. Takagi, and A. Cavalleri, “Light-induced superconductivity in a stripe-ordered cuprate,” *Science* **331**, 189–191 (2011).
- [2] C. R. Hunt, D. Nicoletti, S. Kaiser, T. Takayama, H. Takagi, and A. Cavalleri, “Two distinct kinetic regimes for the relaxation of light-induced superconductivity in $\text{La}_{1.675}\text{Eu}_{0.2}\text{Sr}_{0.125}\text{CuO}_4$,” *Phys. Rev. B* **91**, 020505 (2015).
- [3] S. Kaiser, C. R. Hunt, D. Nicoletti, W. Hu, I. Gierz, H. Y. Liu, M. Le Tacon, T. Loew, D. Haug, B. Keimer, and A. Cavalleri, “Optically induced coherent transport far above T_c in underdoped $\text{YBa}_2\text{Cu}_3\text{O}_{6+\delta}$,” *Phys. Rev. B* **89**, 184516 (2014).
- [4] W. Hu, S. Kaiser, D. Nicoletti, C. R. Hunt, I. Gierz, M. C. Hoffmann, M. Le Tacon, T. Loew, B. Keimer, and A. Cavalleri, “Optically enhanced coherent transport in $\text{YBa}_2\text{Cu}_3\text{O}_{6.5}$ by ultrafast redistribution of interlayer coupling,” *Nat. Mater.* **13**, 705–711 (2014).
- [5] C. R. Hunt, D. Nicoletti, S. Kaiser, D. Pröpper, T. Loew, J. Porras, B. Keimer, and A. Cavalleri, “Dynamical decoherence of the light induced interlayer coupling in $\text{YBa}_2\text{Cu}_3\text{O}_{6+\delta}$,” *Phys. Rev. B* **94**, 224303 (2016).
- [6] M. Mitrano, A. Cantaluppi, D. Nicoletti, S. Kaiser, A. Perucchi, S. Lupi, P. Di Pietro, D. Pontiroli, M. Ricc, S. R. Clark, D. Jaksch, and A. Cavalleri, “Possible light-induced superconductivity in K_3C_{60} at high temperature,” *Nature* **530**, 461–464 (2016).
- [7] A. Pashkin, M. Porer, M. Beyer, K. W. Kim, A. Dubroka, C. Bernhard, X. Yao, Y. Dagan, R. Hackl, A. Erb, J. Demsar, R. Huber, and A. Leitenstorfer, “Femtosecond response of quasiparticles and phonons in superconducting $\text{YBa}_2\text{Cu}_3\text{O}_{7-\delta}$ studied by wideband terahertz spectroscopy,” *Phys. Rev. Lett.* **105**, 067001 (2010).
- [8] S. Dal Conte, C. Giannetti, G. Coslovich, F. Cilento, D. Bossini, T. Abebaw, F. Banfi, G. Ferrini, H. Eisaki, M. Greven, A. Damascelli, D. van der Marel, and F. Parmigiani, “Disentangling the Electronic and Phononic Glue in a High-Tc Superconductor,” *Science* **335**, 1600 (2012).
- [9] S. Kaiser, “Light-induced superconductivity in high-Tc cuprates,” *Physica Scripta* (2017).
- [10] D. Nicoletti, E. Casandruc, Y. Laplace, V. Khanna, C. R. Hunt, S. Kaiser, S. S. Dhesi, G. D. Gu, J. P. Hill, and A. Cavalleri, “Optically induced superconductivity in striped $\text{La}_{2-x}\text{Ba}_x\text{CuO}_4$ by polarization-selective excitation in the near infrared,” *Phys. Rev. B* **90**, 100503 (2014).
- [11] E. Casandruc, D. Nicoletti, S. Rajasekaran, Y. Laplace, V. Khanna, G. D. Gu, J. P. Hill, and A. Cavalleri, “Wavelength-dependent optical enhancement of superconducting interlayer coupling in $\text{La}_{1.885}\text{Ba}_{0.115}\text{CuO}_4$,” *Phys. Rev. B* **91**, 174502 (2015).
- [12] Aavishkar A. Patel and Andreas Eberlein, “Light-induced enhancement of superconductivity via melting of competing bond-density wave order in underdoped cuprates,” *Phys. Rev. B* **93**, 195139 (2016).
- [13] Zachary M. Raines, Valentin Stanev, and Victor M. Galitski, “Enhancement of superconductivity via periodic modulation in a three-dimensional model of cuprates,” *Phys. Rev. B* **91**, 184506 (2015).
- [14] M. Först, A. Frano, S. Kaiser, R. Mankowsky, C. R. Hunt, J. J. Turner, G. L. Dakovski, M. P. Minitti, J. Robinson, T. Loew, M. Le Tacon, B. Keimer, J. P. Hill, A. Cavalleri, and S. S. Dhesi, “Femtosecond x rays link melting of charge-density wave correlations and light-enhanced coherent transport in $\text{YBa}_2\text{Cu}_3\text{O}_{6.6}$,” *Phys. Rev. B* **90**, 184514 (2014).
- [15] M. Forst, C. Manzoni, S. Kaiser, Y. Tomioka, Y. Tokura, R. Merlin, and A. Cavalleri, “Nonlinear phononics as an ultrafast route to lattice control,” *Nat Phys* **7**, 854–856 (2011).
- [16] R. Mankowsky, A. Subedi, M. Forst, S. O. Mariager, M. Chollet, H. T. Lemke, J. S. Robinson, J. M. Glowia, M. P. Minitti, A. Frano, M. Fechner, N. A. Spaldin, T. Loew, B. Keimer, A. Georges, and A. Cavalleri, “Nonlinear lattice dynamics as a basis for enhanced superconductivity in $\text{YBa}_2\text{Cu}_3\text{O}_{6.5}$,” *Nature* **516**, 71–73 (2014).
- [17] Alaska Subedi, Andrea Cavalleri, and Antoine Georges, “Theory of nonlinear phononics for coherent light control of solids,” *Phys. Rev. B* **89**, 220301 (2014).
- [18] M. A. Sentef, A. F. Kemper, A. Georges, and C. Kollath, “Theory of light-enhanced phonon-mediated superconductivity,” *Phys. Rev. B* **93**, 144506 (2016).
- [19] M. Babadi, M. Knap, I. Martin, G. Refael, and E. Demler, “The theory of parametrically amplified electron-phonon superconductivity,” *ArXiv e-prints* (2017), arXiv:1702.02531 [cond-mat.supr-con].
- [20] Y. Murakami, N. Tsuji, M. Eckstein, and P. Werner, “Nonequilibrium steady states and transient dynamics of superconductors under phonon driving,” *ArXiv e-prints* (2017), arXiv:1702.02942 [cond-mat.supr-con].
- [21] M. A. Sentef, “Light-enhanced electron-phonon coupling from nonlinear electron-phonon coupling,” *Phys. Rev. B* **95**, 205111 (2017).

- [22] S. J. Denny, S. R. Clark, Y. Laplace, A. Cavalleri, and D. Jaksch, “Proposed parametric cooling of bilayer cuprate superconductors by terahertz excitation,” *Phys. Rev. Lett.* **114**, 137001 (2015).
- [23] Michael Knap, Mehrtash Babadi, Gil Refael, Ivar Martin, and Eugene Demler, “Dynamical cooper pairing in nonequilibrium electron-phonon systems,” *Phys. Rev. B* **94**, 214504 (2016).
- [24] Dante M. Kennes, Eli Y. Wilner, David R. Reichman, and Andrew J. Millis, “Transient superconductivity from electronic squeezing of optically pumped phonons,” *Nat Phys* **13**, 479–483 (2017).
- [25] S. Kaiser, S. R. Clark, D. Nicoletti, G. Cotugno, R. I. Tobey, N. Dean, S. Lupi, H. Okamoto, T. Hasegawa, D. Jaksch, and A. Cavalleri, “Optical properties of a vibrationally modulated solid state mott insulator,” *Sci. Rep.* **4** (2014), 10.1038/srep03823.
- [26] R. Singla, G. Cotugno, S. Kaiser, M. Först, M. Mitrano, H. Y. Liu, A. Cartella, C. Manzoni, H. Okamoto, T. Hasegawa, S. R. Clark, D. Jaksch, and A. Cavalleri, “THz-Frequency Modulation of the Hubbard U in an Organic Mott Insulator,” *Phys. Rev. Lett.* **115**, 187401 (2015).
- [27] Minjae Kim, Yusuke Nomura, Michel Ferrero, Priyanka Seth, Olivier Parcollet, and Antoine Georges, “Enhancing superconductivity in A_3C_{60} fullerides,” *Phys. Rev. B* **94**, 155152 (2016).
- [28] G. Mazza and A. Georges, “Non-equilibrium superconductivity in driven alkali-doped fullerides,” *ArXiv e-prints* (2017), arXiv:1702.04675 [cond-mat.supr-con].
- [29] J Solyom, “The Fermi gas model of one-dimensional conductors,” *Adv. Phys.* **28**, 201–303 (1979).
- [30] Johannes Voit, “Phase diagram and correlation functions of the half-filled extended Hubbard model in one dimension,” *Phys. Rev. B* **45**, 4027–4042 (1992).
- [31] Johannes Voit, “One-dimensional Fermi liquids,” *Rep. Prog. Phys.* **58**, 977 (1995).
- [32] Martin Eckstein, Marcus Kollar, and Philipp Werner, “Interaction quench in the hubbard model: Relaxation of the spectral function and the optical conductivity,” *Phys. Rev. B* **81**, 115131 (2010).
- [33] Hantao Lu, Shigetoshi Sota, Hiroaki Matsueda, Janez Bonca, and Takami Tohyama, “Enhanced charge order in a photoexcited one-dimensional strongly correlated system,” *Phys. Rev. Lett.* **109** (2012).

Light-induced superconductivity in a strongly correlated electron system: Supplement material

Nikolaj Bittner¹, Takami Tohyama², Stefan Kaiser^{1,3} and Dirk Manske¹

¹*Max-Planck-Institut für Festkörperforschung, D-70569 Stuttgart, Germany*

²*Department of Applied Physics, Tokyo University of Science, Tokyo 125-8585, Japan*

³*4th Physics Institute, University of Stuttgart, D-70569 Stuttgart, Germany*

Phase quench

Dynamical coexistence. Excitation spectrum and correlation function

In Fig. 6 we plot the excitation spectrum after pumping (black line), which show several distinct peaks. The most intensive peaks in the Fourier spectrum can be identified with the initial equilibrium CDW phase. In fact,

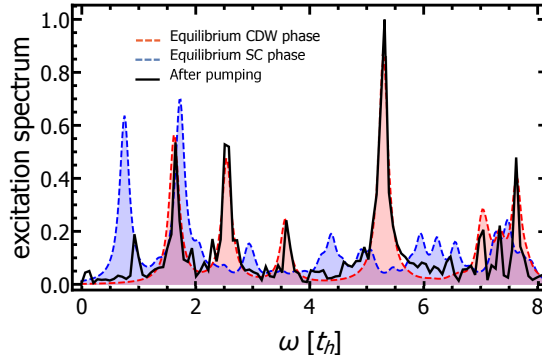


Figure 6. (color online) Excitation spectrum of the system in nonequilibrium (black solid line) compared with the spectra in equilibrium singlet SC phase (blue region) and equilibrium CDW phase (red region).

low energy peaks at $\omega \approx 1.5, 2.5, 3.5$ and 5.5 match perfectly with excitation spectrum for the CDW phase. In addition, a peak at $\omega \approx 1.5$ might also represent an excited state of the singlet superconducting phase, since one of the most intensive peaks in the optical spectrum of the superconducting state appears at the same frequency. Additionally, a peak at $\omega \approx 1$ in the Fourier spectrum can be assigned to the second intensive peak in the spectrum of the superconducting phase. Finally, some less intensive peaks at $\omega \approx 5$ and around $\omega \approx 6$ can be assigned to the superconducting phase.

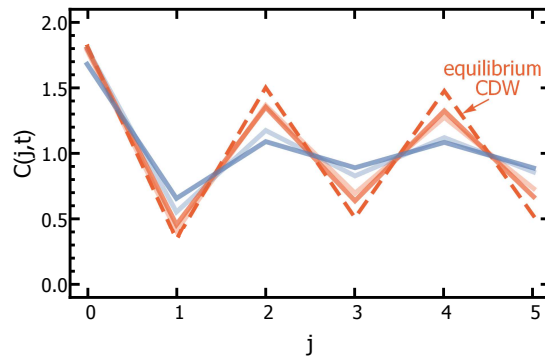


Figure 7. (color online) Time-dependent density-density correlation function $C(j, t)$ as a function of the lattice site j obtained after a pump pulse excitation of the Gaussian shape. The parameters of the pulse are: $A_0 = 5$, $\omega = 2.38$, $\tau = 0.05$. The function $C(j, t)$ is exemplary shown at times: $t = 1$ (light red solid line), $t = 3$ (light blue solid line), $t = 5$ (red solid line), $t = 7$ (blue solid line). For comparison, the correlation function in equilibrium CDW phase is shown by the red dashed line.

To explore temporal evolution of the charged order, we plot in Fig. 7 the time-dependent density-density correlation function $C(j, t)$. Before pumping the electron system is prepared in the equilibrium ground state of the CDW phase and $C(j, t)$ shows a characteristic "zigzag" structure (red dashed line). Clearly, the excitation of the system with the pulse leads to an effective partial suppression of the charge density wave correlations with the subsequent oscillations.

Optical conductivity

Finally, in Fig. 8 we show the time-dependent real part of the optical conductivity $\sigma_1(\Delta t, \omega)$. In agreement with the results for the imaginary conductivity $\sigma_2(\Delta t, \omega)$ [see Fig. 5 in the main text] we observe first a partial reduction of the spectral weight of the low energy peak corresponding to the equilibrium CDW state at both $\Delta t = 1$ (light red solid line) and $\Delta t = 2$ (red solid line) with the appearance of an in-gap state at $\omega \approx 0.7$. At $\Delta t = 3$ the response from CDW is disappeared and the spectral weight is shifted to a low-energy peak at $\omega \approx 0$ representing a transient δ -peak.

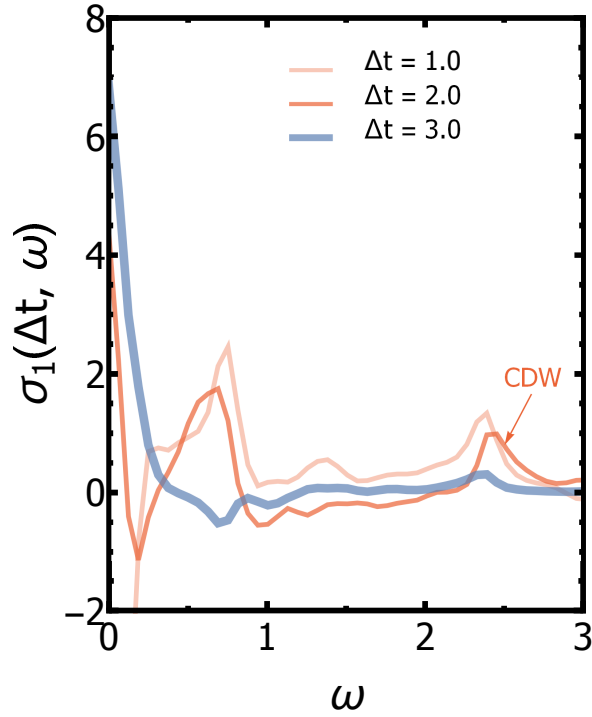


Figure 8. (color online) (a) Time-dependent real conductivity $\sigma_1(\Delta t, \omega)$. Theoretically obtained results at different time delays are presented by the solid lines: $\Delta t=1$ (light red), $\Delta t=2$ (red), and $\Delta t=3$ (blue).